



The interaction of the (7-chloroquinolin-4-yl)-(2,5-dimethoxyphenyl)-aminehydrochloridedihydrate with serum albumin proteins, inputs from spectroscopic, molecular docking and X-ray diffraction studies.

Journal:	<i>RSC Advances</i>
Manuscript ID	RA-ART-02-2015-002815.R1
Article Type:	Paper
Date Submitted by the Author:	16-Sep-2015
Complete List of Authors:	Singh, Shailja; University of Delhi, Chemistry Sharma, Kumkum; University of Delhi, Chemistry Awasthi, Satish; Delhi University, Delhi, Chemistry Department; Delhi University, Chemistry Department
Subject area & keyword:	

Cite this: DOI: 10.1039/c0xx00000x

www.rsc.org/xxxxxx

ARTICLE TYPE

The interaction of the (7-chloroquinolin-4-yl)-(2,5-dimethoxyphenyl)-aminehydrochloridedihydrate with serum albumin proteins, inputs from spectroscopic, molecular docking and X-ray diffraction studies.

Shailja Singh, Kumkum Sharma, Satish K. Awasthi*

5 Chemical Biology Laboratory, Department of Chemistry, University of Delhi, Delhi 110007, India

Received (in XXX, XXX) Xth XXXXXXXXX 20XX, Accepted Xth XXXXXXXXX 20XX

DOI: 10.1039/b000000x

Interaction of (7-chloroquinolin-4-yl)-(2,5-dimethoxyphenyl)-aminehydrochloridedihydrate (CQDPA), amodiaquine analog, a combination partner in antimalarial therapy with serum albumin proteins (BSA and HSA) was carried out using spectroscopic techniques. Fluorescence studies at three different temperatures confirmed binding of CQDPA to the active site of proteins. Thermodynamic properties such as enthalpy change (ΔH^0), Gibbs free energy change (ΔG^0) and entropy change (ΔS^0) suggested that molecule CQDPA binds to site I (subdomain II) of BSA and HSA involving hydrophobic interactions. Based on the Forster's theory of non-radiation energy transfer, the relation of binding average distance r between the donor (BSA & HSA) and acceptor CQDPA was found to be 2.63 and 2.77 for BSA and HSA respectively. CD study reveals that α -helical content remain intact in both BSA and HSA on addition of amodiaquine analogue but with decrease in intensity. The computational analysis and molecular docking of the CQDPA with BSA & HSA also corroborates to the experimental results.

Introduction

Malaria is among one of the most dangerous, infectious diseases on earth since ancient times and human morbidity and mortality is caused by parasite *P. falciparum*. According to the latest report of World Health Organisation, 106 countries are considered endemic for malaria in 2010.¹ Quinoline and its derivatives are well known and widely used antimalarial drugs from past several decades. But appearance of drug resistance into frontline drugs against malaria such as chloroquine, amodiaquine, atovaquone, pyrimethamine and sulfoxadine has warned us for the development of new and more potent antimalarial drugs. In the model list of essential medicines of world health organisation, amodiaquine (AQ) is reintroduced due to its chemical structure.² AQ, a derivative of 4-aminoquinoline is similar to chloroquine in structure and activity and has been used as antimalarial, as well as antipyretic and anti-inflammatory agent.³ Due to the cross-resistance between CQ and AQ, AQ is preferentially in use than chloroquine in areas which are identified as chloroquine resistant. Consequently, AQ was chosen by several countries as the first-line drug in combination with artesunate.⁴ Therefore, there is an urgent need to find new molecules which can substitute amodiaquine with negligible side effects to host and have easy cost effective synthesis. Serum albumins are the most abundant proteins which are responsible for transport of drugs in biological systems and are frequently used in biophysical and biochemical studies to understand the interactions between proteins and small molecules.⁵ These proteins have identical folding structures having three α -helical domains I, II, III in which each domain is further subdivided into A and B which interact with small

molecules. The stereostructure of BSA reveals that it has two tryptophans; Trp134 and Trp 213 which are located in subdomains IA and IIA respectively, while HSA has only one tryptophan residue; Trp 214, present in subdomain IIA.^{6,7} Spectroscopic methods such as UV-visible, fluorescence, circular dichroism have been widely used to understand the interaction between albumin proteins and small molecules or drugs. These interaction mechanisms reveal the accessibility of drugs to albumin's fluorophore which can help us to determine the extent of binding and thus provide information regarding structural changes that determine the therapeutic effectiveness of drugs.⁸⁻¹⁰ In the last few years, our group has focused mainly on design and synthesis of new antimalarials, antifilarials, X-rays analysis of small molecules and development of methodology for tetrazoles synthesis.¹¹⁻¹⁵ Recently, we have evaluated antimalarial compound in vivo with interesting results.¹⁶ To explore new antimalarial molecules, we designed amodiaquine analogue and evaluated in-vitro study (results unpublished). Till now, the specific mode of interaction of such type of amodiaquine derivatives with various albumin proteins has seldom been researched at the molecular level.^{17,18} In this paper, we chose CQDPA molecule to study its interaction with BSA and HSA due to its high antimalarial activity using UV, fluorescence and CD. This study may provide valuable information related the biological effects of AQ and therapeutic effect of this drug in pharmacology and pharmacodynamics. This study will help us to further design new lead molecule based on these observations.

Materials and methods

2.1 Chemicals

Chemicals were analytical grade. Double distilled water was used for all experiments. Bovine serum albumin, human serum albumin, 4, 7-dichloroquinoline, 2,5-methoxy aniline, tris-HCl were purchased from Sigma-Aldrich Chemicals USA. BSA and HSA solutions (1.0×10^{-5} M) were prepared in tris-HCl buffer at pH 7.4 and kept in the dark at 4°C.

2.2 Apparatus and Instruments

The absorption spectra were recorded at room temperature by Specord 250-222P145 UV-vis absorption spectrophotometer equipped with a 1.0 cm quartz cell. Steady state fluorescence emission spectra were recorded on Cary eclipse spectrometer equipped with 1.0 cm quartz cells within 300-500 nm range with the excitation wavelength 280nm ($\Delta\lambda=15$ nm) using 5/5 slit width. The CD measurements were performed on a Jasco-810 automatic recording spectrophotometer using a 10 mm path length at 20°C. The spectra were recorded in the range of 200-300nm. X-ray intensity data were collected on an Oxford Diffraction Xcalibur CCD diffractometer with graphite monochromated Mo K α radiation ($\lambda = 0.71073$ Å) at 293 (2) K. Auto Dock 1.5.6 program was used to realize the binding mode of CQDPA at the active site of HSA and BSA. The crystal structure of BSA and HSA were obtained from the Protein Data Bank (entry code 4F5S and 1E7H). The PyMol molecular graphics system (DeLano Scientific, San Carlos, USA, Version 0.99rc6) was used to delete water molecules from the crystal structure of BSA and visualise the docked conformation. The lowest energy conformation in the largest cluster of each docking simulation was extracted and analyzed. The hydrogen bonds and hydrophobic interactions between the ligands and the protein were represented with Ligplot+ version v.1.4.5 and Viewerlite 4.2.

2.3 Binding parameter

The Stern-Volmer equation (1) was used to understand quenching phenomenon between protein and drug.

$$F_0/F = 1 + K_{sv} \cdot Q = 1 + K_q \cdot \tau_0 \cdot [Q] \quad (1)$$

By using the above equation, the plot was obtained, and the quenching constant (K_{sv}) is defined by the slope of curve. Further, the binding constants can be counted using the modified Stern-Volmer equation as shown below (2):

$$F_0/\Delta F = 1/f_a + 1/(f_a \cdot K_A \cdot [Q]) \quad (2)$$

Where f_a is the fraction maximum fluorescence intensity of protein summed up and K_A is constant. The dependence of $F_0/\Delta F$ on the reciprocal value of quench concentration, $1/[Q]$ is linear with slope equal to the value of $1/f_a K_A$. The value $1/f_a$ is fixed on the ordinate.

According to the Foster energy transfer theory¹⁹ the efficiency of energy transfer E , between the donor the acceptor is defined as in equation (3):

$$E = R_0^6 / (R_0^6 + r^6) \quad (3)$$

Where, R_0 is the Foster radius that yields 50% energy transfer efficiency which can be calculated using equation (4) as given below:

$$R_0^6 = 8.8 \times 10^{-25} (K^2 N^{-4} \Phi J) \quad (4)$$

Where K^2 is the spatial orientation factor of dipole, and N is the refractive index of medium. Φ is the fluorescence quantum yield of donor and J is the overlap integral of the emission spectrum of the donor and absorption spectrum of the acceptor. The overlap integral J can be calculated by using equation (5):

$$J = \int F_D(\lambda) \epsilon(\lambda) \lambda^4 / \int F_D(\lambda) \Delta \lambda \quad (5)$$

Where $F_D(\lambda)$ is the fluorescence intensity of the donor of wavelength, $\epsilon(\lambda)$ is the molar absorption coefficient of acceptor at wavelength, λ , and the efficiency of energy transfer also can be obtained using the equation (6):

$$E = 1 - F/F_0 \quad (6)$$

By means of the above equations, the values of E , R_0 , J and r can be calculated.

Considering that the enthalpy change (ΔH^0) does not vary significantly over this temperature range, its value and that of ΔS^0 can be calculated using the Van't Hoff equation (7):

$$\ln K_A = -(\Delta H^0/RT) + (\Delta S^0/R) \quad (7)$$

The free energy of protein-drug interaction can be calculated from the following equation (8):

$$\Delta G^0 = \Delta H^0 - T\Delta S^0 \quad (8)$$

2.4 Synthesis and crystal growth

The compound CQDPA was synthesized using 4, 7-dichloroquinoline and 2,5-dimethoxy aniline. Briefly, equimolar quantities of 2, 5-dimethoxyaniline (153.18mg, 1mmol) and 4,7-dichloroquinoline (196mg, 1mmol) were refluxed in dry ethanol for 12h. The ligand was purified by successive recrystallization. The pure compound was kept further for crystallization at room temperature. Single crystals of (7-chloroquinolin-4-yl)-(2,5-dimethoxyphenyl)-aminehydrochloridedihydrate were obtained by the slow evaporation of dry ethanol and a crystal of size 25 x 15 x 8 mm³ was selected for X-ray analysis.

3. Results and discussion

3.1 Crystal packing

The compound CQDPA (C₁₈H₁₆Cl₂N₂O₂·2H₂O), crystallized in monoclinic cell setting having P 2₁/n space group as shown in Figure 1. It is clear from the structure that the dimethoxy ring is twisted at an angle of 68.66° with respect to 7-chloroquinoline ring. The molecules are connected through intermolecular hydrogen bonding viz. C7-H7...Cl2 [D=2.868], C5-H5...O3 [D=2.579], N1-H1...Cl2 [D=2.439], C16-H16A...Cl1 [D=2.903], C6-H6...Cl2 [D=2.699] and other short interactions like N2...O4 [D=2.741]²⁰ (Fig. S1, S2). It was found that during the crystallization process, two water molecules and one HCl molecule were co-crystallized along with the desired molecule. These molecules facilitated the crystal packing in three dimensional networks. Data of the crystal are summarized in Table 1 and list of H-bonding are given in Table S1.

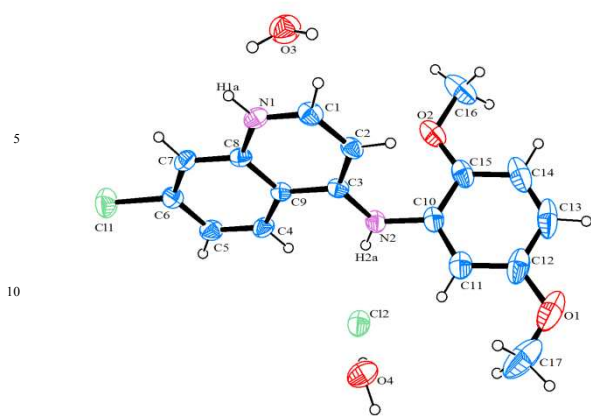


Fig. 1: The molecular structure of 7-(chloroquinolin-4-yl)-(2,5-dimethoxyphenyl)-amine hydrochloride dihydrate (CQDPA) showing 30% probability ellipsoids.

Empirical formula	$C_{17}H_{20}Cl_2N_2O_4$
Formula weight ($\text{g}\cdot\text{mol}^{-1}$)	387.26
Temperature (K)	293(2)
Wavelength (\AA)	0.71073
Crystal system, Space group	Monoclinic, $P 2_1/n$
a (\AA)	7.8844 (10)
b (\AA)	23.029 (2)
c (\AA)	11.0843 (12)
α (deg)	90.00
β (deg)	109.306 (12)
γ (deg)	90.00
Density (g/cm^3)	1.354
Z	4
Reflection/Parameter/Restraints	3926/306/0
Abs coefficient (μ/mm^{-1})	0.365
$F(000)$	808.0
Crystal size (mm^3)	0.50 x 0.30 x 0.10
Goodness-of-fit on F^2	1.093
R_{int}	0.0529
Final R indices [$I > 2\sigma(I)$]	$R_1 = 0.0730$ (2446),
$wR(F^2)$	$wR = 0.1194$ (3926)
Data collection	0.1409
Radiation type	CrysAlisPro
Absorption correction type	Mo $K\alpha$
H-atom treatment	Multi-scan
Refinement method	Mixed
	SHELXL-97
CCDC no	890861

Table 1: Some important crystallographic data and parameter of CQDPA

3.2 Analysis of absorption spectra

The weak absorption peak at $\lambda = 279$ nm appears due to the aromatic amino acids (Trp, Tyr, and Phe).²¹ It is well known that the absorption of a chromophore is shifted in directions and magnitudes that depend on whether it is transferred to a more hydrophilic or more hydrophobic environment. These shifts are

scribed to a change in $\pi-\pi^*$ transition brought about by changes in the polarizability of the solvent.²²

When a molar excess of CQDPA was titrated into a fixed concentration of albumin proteins, a remarkable increase in absorbance intensity of BSA and HSA was observed. The absorption spectra of ligand-BSA and ligand-HSA are shown in Fig. 2 and 3 respectively. In absorption spectra, blue shift was observed both in BSA and HSA on addition of CQDPA suggested that the CQDPA binds to BSA and HSA respectively and the binding is associated with obvious changes in the dielectric environment of residues in serum albumin proteins.

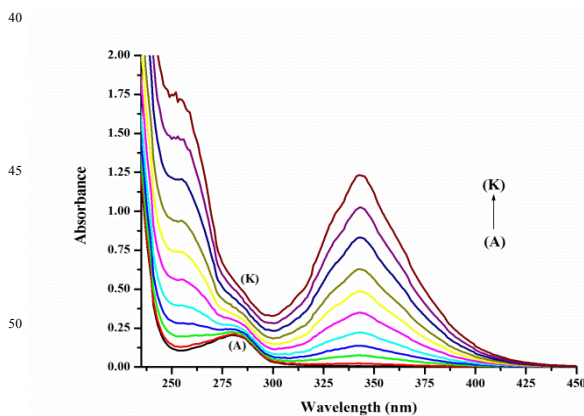


Fig. 2: Absorbance spectrum of BSA-CQDPA. $[C_{\text{BSA}}] = 10 \times 10^{-6} \text{ mol L}^{-1}$; (A) $C_{\text{BSA}}/C_{\text{CQDPA}} = 1/0$; (I) $C_{\text{BSA}}/C_{\text{CQDPA}} = 1/10$ (288 K, pH=7.40).

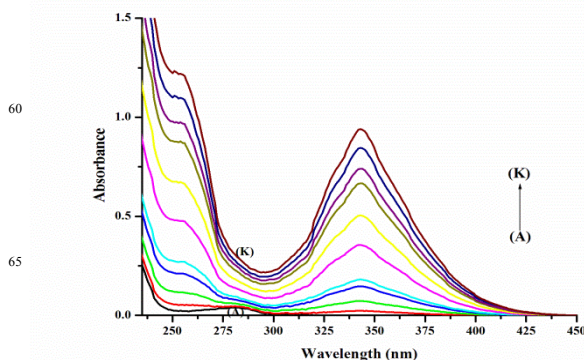


Fig. 3: Absorbance spectrum of HSA-CQDPA. $[C_{\text{HSA}}] = 10 \times 10^{-6} \text{ mol L}^{-1}$; (A) $C_{\text{BSA}}/C_{\text{CQDPA}} = 1/0$; (I) $C_{\text{HSA}}/C_{\text{CQDPA}} = 1/10$ (288 K, pH=7.40)

3.3 Analysis of fluorescence spectra

Fluorescence is one of the most powerful techniques to study interaction of small molecules with proteins. Such study gives an idea about binding mechanism, mode of binding and binding sites in protein and small molecules. Fig. 4 illustrates the emission spectra of BSA and HSA in presence of various concentrations of CQDPA. The fluorescence emission wavelength of both BSA and HSA is about 350 nm which is characteristic of partial shielding of the tryptophan residues in aqueous solvent. It is apparent from the figure 4 that fluorescence intensity of albumin proteins decreased gradually with the increase in CQDPA concentration, implying that the binding of CQDPA to BSA and HSA occurred and the microenvironment around chromophores of albumin proteins had been changed. Further, fluorescence emission

wavelengths of BSA showed red shifts on addition of the molecule, which indicated that the tryptophan and tyrosine residues in protein are located near hydrophobic environment as reported earlier.²² While, in the case of HSA (Fig.4, inset) we could see a blue shift which suggests the presence of binding site in hydrophilic centre. These changes also indicated that the CQDPA strongly interact with the site adjacent to the tryptophan residues in protein.²³ This is in agreement with the results of UV-vis experiments.

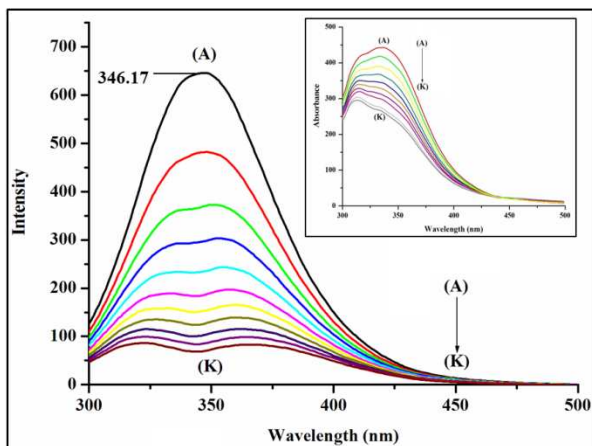


Fig. 4: Fluorescence emission spectrum of BSA and HSA (inset) in absence and presence of CQDPA. (A) $\lambda_{\text{ex}}=280$ nm $C_{\text{BSA}}=10 \times 10^{-6}$ mol L⁻¹ (A-K)=1/0-1/10, respectively (288 K, pH=7.40).

The accessibility of the fluorophores to quencher was realised through quenching experiments and the corresponding Stern-Volmer plots. The Stern-Volmer equation is always used to define the mechanism of the fluorescence quenching. It is well documented that static quenching results from the formation of a non-fluorescent fluorophore-quencher complex, formed in the fluorophore's ground state, while the dynamic quenching is derived from the collisions.

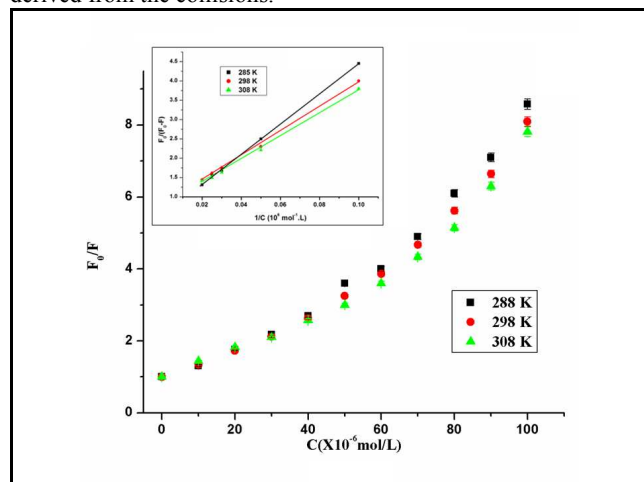


Fig. 5: Stern-Volmer curves of the fluorescence quenching of BSA at different temperature (■ 288 K, ● 298 K, ▲ 308 K); (inset): Modified Stern-Volmer plots of BSA on different temperature. $\lambda_{\text{ex}}=280$ nm, pH=7.4. (■ 288 K, ● 298 K, ▲ 308 K).

From figure 5, the linearity of Stern-Volmer of BSA came out to an upward curvature when the concentration ratio was more than 4, while there was good linearity when $C_{\text{ligand}}/C_{\text{BSA}} \leq 4$, that is to say, at the low concentration of CQDPA, thus, a single quenching mechanism existed in the binding process. But as the temperature increased both dynamic and static quenching occurred, since higher temperature resulted in faster diffusion & larger amount of collisional quenching occurs.

From the plot of Stern-Volmer, the value of K_{SV} was obtained and given in Table 2. $K_{\text{SV}} = 3.98 \times 10^5$ mol L⁻¹. It is well known that $K_{\text{SV}} = Kq \cdot \tau_0$, where Kq is the quenching rate constant and τ_0 is the fluorescence lifetime of protein in the absence of quencher; the value of τ_0 is considered to be 10^{-8} s.³ Therefore, the value of Kq was obtained, $Kq = 3.98 \times 10^{13}$ mol L⁻¹s⁻¹, which is greater than the optical collision constant, 2×10^{10} mol L⁻¹s⁻¹.^{24, 25} It suggested that the fluorescence decay was not a process of dynamic quenching but due to static quenching at low concentrations of small molecule.

When the concentration ratios were higher than 4, the plot appears to be an upward curvature with the increasing small molecule concentration, which is the characteristic feature for mixed quenching of combined quenching and/or additional binding sites for high CQDPA.

Mechanism and binding constants could be accurately obtained according to the modified Stern-Volmer equation [2] as shown Fig. 5(inset) for BSA and Fig. 6(inset) for HSA, respectively.

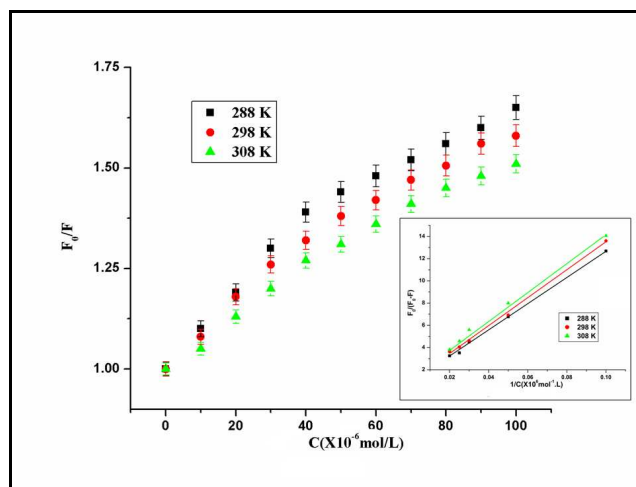


Fig. 6: Stern-Volmer curves of the fluorescence quenching of HSA on the different temperature. (■ 288 K, ● 298 K, ▲ 308 K); (inset): Modified Stern-Volmer plots of HSA on different temperature. $\lambda_{\text{ex}}=280$ nm, pH = 7.40. (■ 288 K, ● 298 K, ▲ 308 K).

On the other hand, in the case of HSA, initially there is a good linearity in Stern-Volmer plot but after $C_{\text{ligand}}/C_{\text{HSA}} \geq 3$ comes out to a downward curvature (Fig. 6). A linear Stern-Volmer plot is generally indicative of a single class of fluorophores and all are equally accessible to quencher. If two fluorophores are present and one class is not accessible to quencher then the Stern-Volmer plots deviates from linearity towards the x-axis. So we concluded that there was a static quenching but all the fluorophores were not equally available to quencher molecules. CQDPA does not readily penetrate the buried hydrophobic interior of proteins and only surface tryptophan residues were quenched. The binding parameters of HSA-ligand are summarised in Table 3.

pH	T (K)	K_{sv} ($\times 10^5 \text{Lmol}^{-1}$)	K_A ($\times 10^5 \text{Lmol}^{-1}$)	ΔG^0 (kJmol^{-1})	ΔH^0 (kJmol^{-1})	ΔS^0 ($\text{Jmol}^{-1}\text{K}^{-1}$)
7.4	288	3.98	5.7	-38.60	-3.34	33.40
7.4	298	3.16	5.2	-39.10	-3.34	33.40
7.4	308	2.97	4.9	-39.57	-3.34	33.40

Table 2: The binding parameters of the binding of (7-chloroquinolin-4-yl)-(2,5-dimethoxyphenyl)-amine and BSA (pH = 7.40, λ_{ex} =295 nm)

pH	T (K)	K_{sv} ($\times 10^5 \text{Lmol}^{-1}$)	K_A ($\times 10^5 \text{Lmol}^{-1}$)	ΔG^0 (kJmol^{-1})	ΔH^0 (kJmol^{-1})	ΔS^0 ($\text{Jmol}^{-1}\text{K}^{-1}$)
7.4	288	14.4	3.7	-30.78	-2.50	42.31
7.4	298	12.3	3.4	-31.29	-2.50	42.31
7.4	308	11.7	2.8	-31.79	-2.50	42.31

Table 3: The binding parameters of the binding of (7-chloroquinolin-4-yl)-(2,5-dimethoxyphenyl)-amine and HSA (pH = 7.40, λ_{ex} =295 nm)

It is clear from Table 2 & 3 that Stern-Volmer constant decreased with the increase in temperature, which indicated that interaction between CQDPA and albumin proteins became weaker with the increase in temperature and thus, CQDPA could be transported by BSA in the body.

In the body, several factors like hydrophobic interaction, hydrogen bond, electrostatic interaction, van der Waals force act between small molecules and albumin protein. To determine the exact mode of interactions, thermodynamic parameters were calculated using equation [7] and [8] as shown in Fig. S3.

It is evident from Table 2 & 3 that the negative values of ΔG^0 and ΔH^0 along with the positive values of ΔS^0 were obtained for the CQDPA-BSA & HSA interaction. Negative values of ΔG^0 indicated the spontaneity of the binding process. A positive value of ΔS^0 (33.40 and $42.31 \text{Jmol}^{-1}\text{K}^{-1}$ for BSA and HSA, respectively) indicated hydrophobic interaction. The negative ΔH^0 values (-3.34 and -2.50kJ mol^{-1} for BSA and HSA, respectively) indicated that binding could not be mainly attributed to electrostatic interactions since for electrostatic interactions ΔH^0 remains very small or almost zero. Negative ΔH^0 value would be obtained whenever a hydrogen bond existed in the binding reactions. Furthermore, it is suggested that the ΔG^0 value was derived from a large contribution of the ΔS^0 with a small contribution from the ΔH^0 , so we could interpret that interaction was mainly hydrophobic, but the role of hydrogen bonding could not be neglected.

3.4 The conformation study of BSA and HSA

Circular dichroism spectra are most frequently used to monitor the conformational changes of serum albumin proteins upon addition of drug molecules. It is well documented that native BSA and HSA exhibits two negative bands at 208 and 222 nm, which is a characteristic of α -helical structure of protein.²⁶ The CD spectra of BSA & HSA in absence and presence of compound CQDPA were found similar in shape with peak at position 208 nm and 222 nm. Further, the α -helix content of BSA and HSA decreased with increase of CQDPA concentration as seen by decrease in the negative ellipticity at 222 and 208 nm (Fig. 7). This suggests that there is slight decrease in α -helix content in BSA & HSA upon the addition of CQDPA.

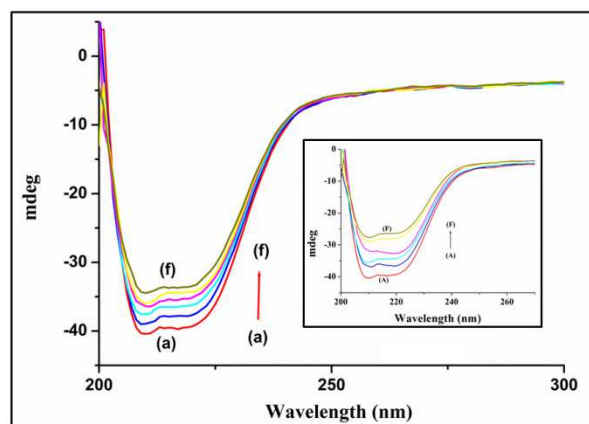


Fig. 7: CD spectrum of BSA in absence and presence of CQDPA. [$C_{BSA}=10 \times 10^{-6} \text{molL}^{-1}$; $C_{BSA}/C_{CQDPA}=1/0-1/1$ (288 K, pH = 7.40); (inset): CD spectrum of HSA in absence and presence of CQDPA. [$C_{HSA}=10 \times 10^{-6} \text{molL}^{-1}$; $C_{HSA}/C_{CQDPA}=1/0-1/1$ (288 K, pH = 7.40)]

The α -helix contents of BSA were calculated from MRE values at 208 nm using the following equation.²⁷

$$\alpha\text{-helix (\%)} = \{(-[\theta]_{208} - 4000) / (33000 - 4000)\} \times 100$$

Where $-\theta_{208}$ is the observed MRE value at 208 nm, 4000 is the MRE of the α -form and random coil conformation cross at 208 nm, and 33000 is the MRE value of a pure α -helix at 208 nm. According to the above equation, the percentage of α -helix of BSA and HSA was calculated. It is found that α -helix decreased from 28.9 ± 0.2 , 28.1 ± 0.1 , 27.2 ± 0.1 , 26.7 ± 0.2 , 26.3 ± 0.3 and $26.0 \pm 0.01\%$ in BSA and 29.6 ± 0.3 , 28.1 ± 0.2 , 27.4 ± 0.1 , 26.6 ± 0.5 , 25.3 ± 0.3 and $24.5 \pm 0.4\%$ in HSA with increasing molar concentration ratio of CQDPA (1:0.0, 1:0.2, 1:0.4, 1:0.6, 1:0.8, 1:1). It is evident from the CD data that increase of concentration of CQDPA perturbs structure of protein but still retain the α -helical structure. Further, the CD spectra of Bovine and human serum albumin in the absence and presence of CQDPA are similar in shape indicating that denaturation did not occur and proteins retained their original nature but slight decrease in α -helicity. The results are well in agreement with the previously reported results of UV-Visible and fluorescence experiments.

3.5 Energy Transfer Study

In general, energy transfer between small molecules and bio-macromolecules have been widely used to understand protein-small molecule interaction and conformational changes in protein conformation.²⁸ According to Forster theory, the energy transfer will take place under the following conditions:

- The donor molecule can produce fluorescent light.

- b) Fluorescence emission spectrum of donor and UV absorption spectrum has more overlap.
- c) The distance between the donor and the approaching acceptor is less than 7nm.

The energy transfer phenomenon is dependent not only to the distance between the acceptor and donor but also to the critical energy transfer distance R_0 and the efficiency of energy transfer E . The value of energy transfer E , can be calculated using equation [3] & [6], while, the overlap integral J can be calculated from the degree of overlap between donor and acceptor using equation [5]. Fig. 8-9 showed the overlap between the absorbance spectrum of CQDPA and BSA & HSA, respectively. The values are documented for BSA, $k^2 = 2/3$, $\Phi = 0.10$, $N = 1.46$ and for HSA, $k^2 = 2/3$, $\Phi = 0.118$, $N = 1.336$.^{29,30} Using these data, we calculated the value of R_0 (2.20 and 2.28 for BSA and HSA, respectively) and r (2.63 and 2.71 for BSA and HSA, respectively) for both bovine serum albumin and human serum albumin respectively.

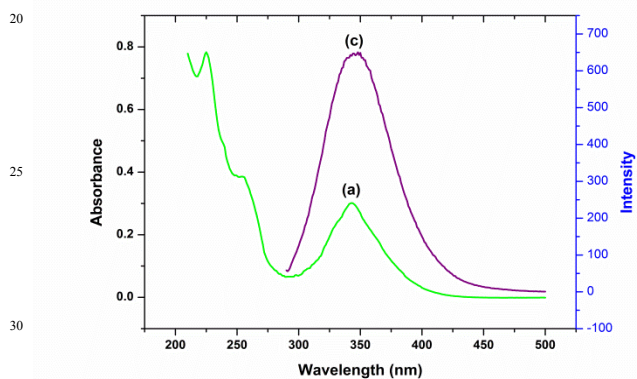


Fig. 8: The overlap of (a) Absorbance spectrum of CQDPA and (b) Fluorescence emission spectrum of BSA. $C_{BSA}/C_{CQDPA} = 1$ (288 K, pH=7.40, $\lambda_{ex}=280$ nm)

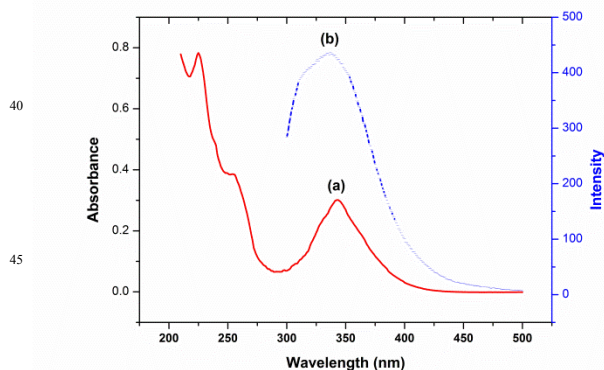


Fig. 9: The overlap of (a) Absorbance spectrum of CQDPA and (b) Fluorescence emission spectrum of HSA. $C_{HSA}/C_{CQDPA} = 1$ (288 K, pH=7.40, $\lambda_{ex}=280$ nm)

3.6 Computational methodology

Theoretical studies on CQDPA were carried out in gas phase using Gaussian 03 programme. The highest occupied molecular orbitals (HOMO) and lowest unoccupied molecular orbital (LUMO) were calculated at B3LYP/6-31+G(d) level of theory

using the optimized geometries at the same level of theory.³¹ Gauss-View 3.0 was used to visualize program to construct the shape of the frontier molecular orbitals. Fig. 10 shows that the most of the electron density is localized on both the phenyl ring and naphthyl ring in HOMO, whereas in LUMO, it is localized on only naphthyl ring. The energy gap between HOMO and LUMO is 5.047455 eV.

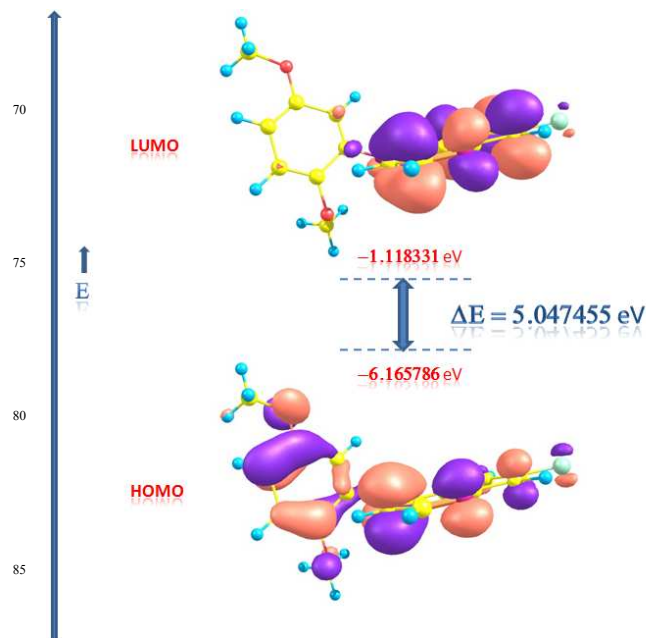


Figure 10. Frontier molecular orbital diagram of compound CQDPA calculated at B3LYP/6-31+G(d) level

3.7 Docking results

The ligand was docked to serum albumin proteins to study the effective interaction of the drug with various amino acid residues in the active site. The most common active site for drug interactions is present in sub-domain IIA i.e., Sudlow's site I.^{32,33} We, therefore, used the Sudlow's site I as an active site for docking of CQDPA. Each grid computation was performed with a grid box of $60 \times 60 \times 60 \text{ \AA}^3$ with 0.375 \AA spacing, which covered the active site residues and allowed for the flexible rotation of the ligand. For rigid docking simulations, the parameters were set to 100 GA runs and terminated after a maximum of 2,500,000 energy evaluations, the population size was set to 150 with a crossover rate of 0.8 (Lamarckian Genetic Algorithm). The predicted binding affinities of BSA and HSA with optimized structure of CQDPA are -6.68 and -5.9 Kcal/mol, respectively. The results imply that CQDPA was bound to Sudlow's site I (subdomain IIA) of BSA where the Trp213 residue is located. Within the docking binding sites of CQDPA, there were possible hydrogen bond interactions between the ring N of CQDPA and Asp108 (3.74 \AA); Cl of CQDPA and Arg144 (3.25 \AA); bridge NH of CQDPA and Ala193 (3.35 \AA); bridge NH of CQDPA and Ser192 (2.66 \AA); between the O-2 of $-\text{OCH}_3$ (at C-17) of CQDPA and Arg458 (3.15 \AA) of BSA. In addition, residues Ser109, Pro110, His145, Leu189, Thr190 and Arg196 provide extra hydrophobic force to stabilize the CQDPA-BSA complex (Fig. 11).

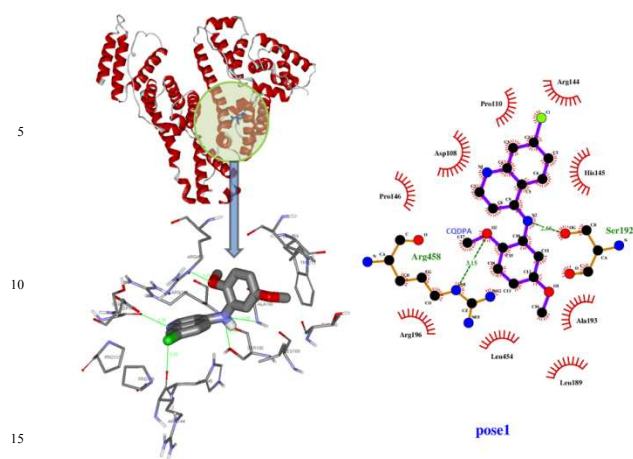


Fig 11: The cartoon representation of the ligand docked to that particular BSA (PDB entry 4F5S) model.

Interestingly, the binding site of CQDPA in HSA is found similar as seen in BSA but with different amino acids. Five hydrogen bond interactions exist between Cl of CQDPA and Ala 215 (3.87 Å), the ring N of CQDPA and Arg 218 (3.38 Å), between the ring N of CQDPA and Leu 219 (3.13 Å); the O-2 of -OCH₃ (at C-17) and Arg 257 (3.86 Å); and the O-1 of -OCH₃ (at C-16) and Ile 290 (3.24 Å). Hydrophobic residues such as Lys199, Phe 211, Trp 214, Arg 222, Phe 223, Leu 238, Val 241, His 242, Leu 260, Ile 264, Ser 287, Ala 291 and Glu 292 surround CQDPA could enhance the binding affinity of CQDPA with HSA (Fig. 12).

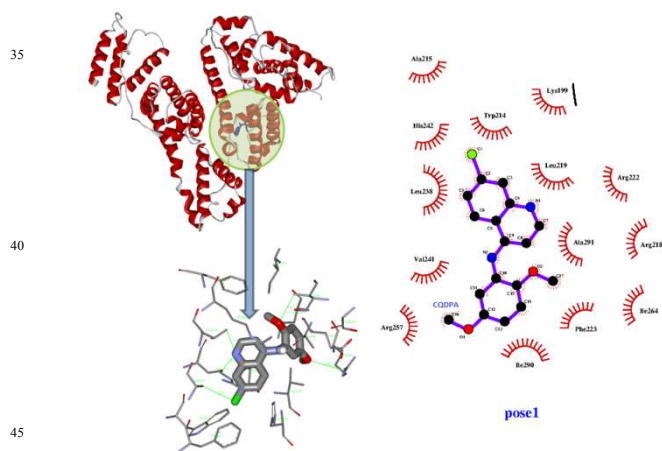


Fig 12: The cartoon representation of the ligand docked to that particular HSA (PDB entry 1E7H) model.

Conclusions

We successfully studied the interaction between (7-chloroquinolin-4-yl)-(2,5-dimethoxyphenyl)-amine hydrochloride dihydrate and serum albumin proteins (BSA & HSA) by UV-visible, fluorescence spectroscopy & circular dichroism methods. The results show that the CQDPA binding to

protein is spontaneous and hydrophobic interactions play an important role in binding. Further, the binding site was located in the micro environment of Trp 213 and Trp 214 of BSA and HSA, respectively. These experimental data are further assisted by molecular docking results. Further, CD studies confirm that ligand interact with BSA as well as HSA without the change in the α -helical structure. These results provide an important insight into the interaction of substituted 4-aminoquinolines with serum albumins which could be very useful in biochemistry and pharmacy.

Acknowledgements

This work was supported by the University Grant Commission, (UGC) (Scheme no 37-410/2009) New Delhi, India, and in part the University of Delhi, Delhi, India. SS and KS are thankful to UGC for financial support. SKA is thankful to the University Sophisticated Instrument Centre (USIC), University of Delhi, India for NMR and X-rays analysis.

Notes and references

- World Health Organisation, World Malaria Report 2010 (2010) available at: <http://www.who.int/malaria/publications/atoz/9789241564106/en/index.html>
- Guglielmo S, Bertinaria M, Rolando B, Crosetti M, Fruttero R, Yardley V, Croft SL, Gasco A, *Eur. J. Med. Chem.*, 2009, **44**, 5071-5079.
- Olliaro P, Nevill C, LeBras J, Ringwald P, Mussano P, Garner P, Brasseur P, *The Lancet*, 1996, **348**, 1196-1201.
- World Health Organisation, Global Report on Antimalarial Drug Efficacy and Drug Resistance: 2000-2010 (2010) pp. 30.
- Carter DC, Ho JX, *Adv. Protein Chem.* 45 (1994) 153-203.
- He XM, Carter DC, *Nature*, 1992 (London), 358, 209; Brown JR, Shockley P, *Lipid-Protein interactions*, 1982, **1**, Wiley New York, 25-68.
- Peters T, *Adv. Protein Chem.*, 1985, **37**, 161-245.
- Tiana J, Zhaob Y, Liua X, Zhaoa S, *Luminescence*, 2009, **24**, 386-393.
- Abdollahpour N, Asoodeh A, Saberi MR, Chamani J, *Luminescence*, 2011, **131**, 1885-1899.
- Tarushi A, Raptopoulou CP, Psycharis V, Terzis A, Psomas G, D.P.Kessissoglou, *Bioorg. Med. Chem.*, 2010, **18**, 2678-2685.
- Mishra N, Arora P, Mishra B, Mishra LC, Bhattacharya A, Awasthi Satish K, Bhasin VK, *Eur. J. Med. Chem.*, 2008, **43**, 1530.
- Yadav N, Dixit SK, Bhattacharya A, Mishra LC, Awasthi, Bhasin VK, *Chemical biology and drug design*, 2012, **80**, 340-347.
- Awasthi SK, Mishra N, Dixit SK, Alka, Yadav M, Yadav SS, Rathur S, *Am. J Trop. Med. & Hyg.*, 2009, **80**, 764.
- Singh S, Singh M, Agarwal A, Awasthi SK, *Acta Cryst.*, 2011, **E67**, o3163.
- Singh S, Singh M, Hussain F, Agarwal A, Awasthi SK, *Acta Cryst.*, 2011, **E67**, o1616-o1617.
- Agarwal D, Sharma M, Dixit SK, Dutta RK, Singh AK, Gupta RD, Awasthi SK, Agarwal et al. *Malarial Journal*, 2015, **14**:48, 1-8
- Samari F, Shamsipur M, Hemmateenejad B, Khayamian T, Gharaghani S, *Eur. J. Med. Chem.*, 2012, **54**, 255-263.
- Viola G, Salvador A, Ceconet L, Basso G, Vedaldi D, Acqual F Dall', Aloisi GG, Amelia M, Barbafrina A, Latterini L, Elisei F, *Photochem. Photobiol.*, 2007, **83**, 1415-1427.
- Forster T, Sinanoglu O, (eds). *Modern Quantum Chemistry*, Academic Press, New York, 1966, **3**, 93.
- Desiraju GR, Steiner T, *The Weak Hydrogen Bond in Structural Chemistry and Biology*, Oxford University Press, 2011.

-
- 21 Lakowicz JR, Weber G, *Biochemistry*, 1973, **12**, 1-61; Lakowicz J
R, *Principles of Fluorescence Spectroscopy*, 2nd edn. Klawer
Academic: New York, 1999.
- 22 Wen MG, Zhang XB, Tian JN, Ni SH, Bian HD, Huang YL, Liang
H, *J. Solution Chem.*, 2009, **38**, 391-401.
- 5 23 Wang YQ, Zhang HM, Zhang GC, Tao WH, Tang SH,
Luminescence, 2007, **126**, 211-218.
- 24 Eftink MR, Ghiron CA, *Anal. Biochem.*, 1981, **114**, 199-227.
- 25 Belletete M, Lachapelle M, Durocher G, *J. Phys. Chem.*, 1990, **94**,
7642-7648.
- 10 26 Zhang X, Lin Y, Liu L, Lin C, *Luminescence*, 2015, **30**, 269-279.
- 27 Greenfield N, Fasman GD, *Biochemistry*, 1969, **8**, 4108-4116.
- 28 Mallick A, Haldar B, Chattopadhyay N, *J. Phys. Chem. B.*, 2005,
109, 14683-14090.
- 15 29 Forster T, In *Modern Quantum Chemistry*; Academic Press: New
York, 1996, 93-137.
- 30 Valeur B, Brochon J.C, *New Trends in Fluorescence Spectroscopy*;
Springer Press: Berlin, Germany, 2001, 25.
- 20 31 Suresh Kumar GS, Prabhu AAM, Bhuvanesh N, Ronica XAV,
Kumaresan S, *Spectrochimic Acta Part A: Molecular and
Biomolecular Spectroscopy*, 2014, **132**, 465-476.
- 32 Maidul H, Asma YK, Gopinatha SK, *Plos One*, 2011, **6**, e26186,
- 33 Zhang X, Li L, Xu Z, Liang Z, Su J, Huang J, Li B, *Plos One*,
25 2013, **8**, e59106